Keysight Technologies

Determining the Elastic Modulus of Thin Films: A Comparative Study of Substrate Accounting and Back Extrapolation

Application Note

KEYSIGHT TECHNOLOGIES

Abstract

Two approaches for determining the elastic modulus of thin films are compared by means of finite-element modeling. The first approach, termed "substrate accounting," applies an analytic model to substrate-affected modulus in order to determine and extract the influence of the substrate, thus isolating the elastic modulus of the film. The second approach, termed "back extrapolation," extrapolates substrate-affected modulus to zero penetration depth in order to determine film modulus at a position that is theoretically free of substrate influence. If the film is mechanically uniform, then both approaches return film modulus with similar accuracy—within 2% for $0.2 < E_f/E_s < 5$. However, if the film has a "skin"—a thin superficial layer which is mechanically different from the rest of the film—then the substrate-accounting approach adds value, because it more clearly reveals the presence of the skin, and because it returns the modulus of the "bulk" of the film with better accuracy than the back-extrapolation approach.

Introduction

The problem of determining intrinsic film properties from indentation data that are influenced by both film and substrate is an old one. If the film is thick enough to be treated as a bulk material, then the analysis of Oliver and Pharr is typically used. [1] But with the decreasing scale of materials, especially in the semiconductor industry, it is often the case that results at all practical indentation depths are substantially affected by the substrate. In 2011, Hay and Crawford introduced an analytic model for accounting for substrate influence on the elastic modulus measured by instrumented indentation. [2,3] Because the model is simple and works well whether the film is stiffer or more compliant than the substrate, it has been widely adopted.

The Hay-Crawford model is used in the following way. First, the elastic modulus is measured according to the method of Oliver and Pharr; this "apparent elastic modulus" is assumed to be substantially influenced by BOTH film and substrate. The Hay-Crawford model is used to predict the magnitude of the substrate influence and then extract the intrinsic (substrate-independent) elastic modulus of the film. Hereafter, the term *substrate accounting* shall refer to the approach of determining the film modulus by accounting for substrate influence using the Hay-Crawford model.

However, an alternate approach to the Hay-Crawford model is described in ISO 14577-4. ISO 14577 is an international standard which governs thin-film testing; Part 4 states that substrate-independent elastic modulus should be determined by measuring the elastic modulus according to the method of Oliver and Pharr over a range of penetration depths and then linearly extrapolating these results back to zero displacement, where substrate influence is theoretically nil. [4] Specifically, ISO 14577-4 requires that at least 15 measurements to at least three different depths be included in the extrapolation. The range for these measurements is specified in terms of the ratio of contact radius to film thickness (a/t). For soft/ductile films, the measurements must all be within the range of $a/t < 1.5$. For hard/brittle films, the measurements must all be within the range of $a/t < 2$. Hereafter, the term back extrapolation shall refer to the approach of determining film modulus by linearly extrapolating apparent modulus, measured over a range of displacements, back to zero displacement according to the prescription of ISO 14577-4.

The purpose of the present work is to compare these two approaches with respect to their effectiveness in returning the elastic modulus of the film. Finite-element analysis (FEA) is the ideal tool for critically comparing these two approaches, because the true film modulus is known—it is an input to the simulation. For example, an elastic finite-element model may be constructed with a film of thickness t on a substrate, with the input properties being the Young's modulus and Poisson's ratio of the film (E_f, υ_f), and the Young's modulus and Poisson's ratio of the substrate (E_S, υ_S). Then, indentation into the material is simulated, and the resultant force-displacement data are analyzed according to both of the approaches we wish to compare: substrate accounting and back extrapolation. Each of these two approaches will yield a value for the Young's modulus of the film. Which approach yields an output value which is closer to the known input value? Finite-element analysis allows this question to be answered systematically over the domain of situations that might be encountered experimentally.

At the outset, fundamental differences between these two approaches should be highlighted, because these differences guided the design of the present investigation:

1. The aims of the two approaches are fundamentally different. The aim of the substrate-accounting approach is to account for the influence of the substrate in order to know the modulus of what remains, which is the film. The aim of the back-extrapolation approach is to achieve a single value for film modulus. If the film is mechanically uniform, then these two aims converge. But if the film is not mechanically uniform, the aims diverge. The substrate-accounting approach aims to determine film modulus apart from substrate influence, even if this film modulus is not uniform. The back-extrapolation approach aims to determine a single value of modulus that is most representative of the film.
2. The substrate-accounting approach yields a value for film modulus for every single test. That is, every measurement of apparent modulus yields a corresponding measure of film modulus. With the back-extrapolation approach, multiple measurements of apparent modulus are required to achieve a single value of film modulus.

At first glance, the first difference identified above may seem unimportant. But experimentally, it is quite common to encounter situations in which the surface of a film is mechanically different from the rest of the film. Reasons for such differences include sample preparation (polishing), environmental exposure (oxidation, water absorption), graded curing, surface tension, etc. Rarely does the experimenter have a *priori* information about such superficial differences. Thus, three sets of finite-element simulations were performed in this work. In the first set of simulations, both film and substrate were mechanically uniform. In the second and third sets of simulations, the film was given a "skin"—a superficial layer which had a modulus of either half or double that of the rest of the film. The thickness of the skin was 1% of the film thickness, and the smallest indentation depth (h) was at least

three times greater than the skin thickness. The purpose of the "skin" simulations was to critically evaluate the two approaches when, unbeknownst to the experimenter, the surface of the film is mechanically different from the rest of the film.

Finite-element Modeling

Three sets of 56 axisymmetric finite-element simulations were performed using Cosmos 2.8. All simulations are summarized in Table 1. All 168 simulations had these inputs in common:

- All materials in the finite-element model were linearly elastic, requiring only an elastic modulus and Poisson's ratio for complete specification.
- The indenter tip was a cone having an included angle of 140.6° and a tip radius of 50nm. The elastic modulus and Poisson's ratio of the indenter tip were 1140GPa and 0.07, respectively.
- All films had a total thickness of t = 500nm. If the film included a skin, then the thickness of the skin was 5nm, and the thickness of the rest of the film was 495nm.
- The elastic modulus and Poisson's ratio of the film were 10GPa and 0.25, respectively.

The following inputs were systematically varied:

- In the first set of 56 simulations, the film was uniform. In the second set of 56 simulations, the film was given a 5nm skin having a modulus of 5GPa (half that of the film). In the third set of 56 simulations, the film was given a 5nm skin having an elastic modulus of 20GPa (double that of the film).
- To achieve the desired variation in E_f/E_s, the substrate modulus varied between 100GPa (E_f/E_s = 0.1) and 1GPa (E_f/E_s = 10).
- To achieve the desired range of a/t, the indentation depth varied from 15nm to 50nm in increments of 5nm.

The purpose of simulations 25–32 was to vet the finite-element model. For these simulations, the finite-element model had the mesh of a film-substrate system, but with film and substrate having the same modulus (i.e. $E_f = E_s$ =10GPa), and so behaving as a bulk sample. Thus, the intention was to verify the general finite-element model by showing that for simulations 25–32, standard analysis of simulated data yields an output modulus that is very close to the input value.

For all simulations, both the indenter and the sample were meshed with four-node axisymmetric plane-strain elements. The mesh was appropriately scaled according to the specified indentation depth. For the sample, the extent of the mesh was 90a' in both the radial and axial directions, where a', the anticipated contact radius, was calculated as the radius of the indenter at a distance from the apex that is equal to the specified indentation depth. The radial extent of the fine mesh near the contact was 1.2a'. The radial extent of the indenter mesh was 45a', and the axial extent was 90a'.

For all simulations, the boundary conditions were specified as follows. Along the right-hand side and bottom of the sample, all nodes were rigidly fixed. Along the axis of symmetry (the left hand side of both the indenter and sample), nodes were constrained to move along the axis of symmetry only (u_x = 0). Nodes along the top of the indenter were displaced downward by the total prescribed displacement which took place in discrete time steps. Nodes along the right-hand side of the indenter were unconstrained, thus allowing the indenter to move as a free body into the sample surface. The interaction between the indenter and the sample was handled as follows. The nodes along the indenter form a curve. Surface nodes on the sample were not allowed to pass to the other side of this curve (line-contact formulation). The contact was frictionless. Finally, no slip was allowed between film and substrate. These prescriptions are typical for finite-element models of indentation experiments.

An updated Lagrangian formulation was used to handle potentially large strains. The solution was achieved in discrete time steps. At each time step, the solution was found by force control with Newton-Raphson iteration.

Figures 1 and 2 show the finite-element mesh at maximum deformation for runs 57 and 64, respectively. The indenter mesh is shown in blue, the skin mesh is shown in aqua, and the film is shown in red. (The substrate is not visible in these figures.)

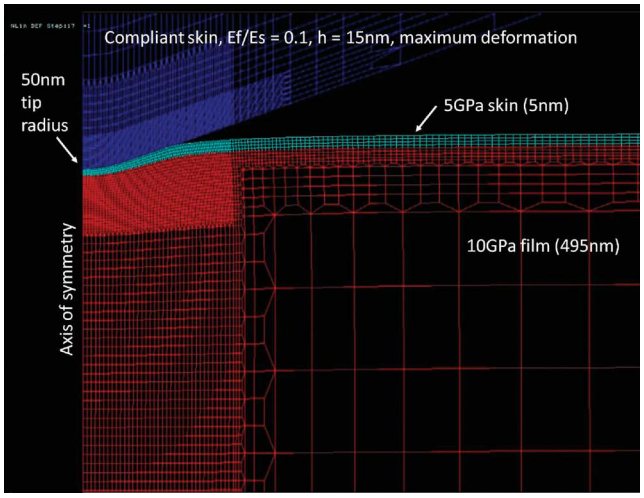

Figure 1. Deformed mesh for simulation 57. Indenter is blue, skin is aqua, and film is red. Substrate is not visible.

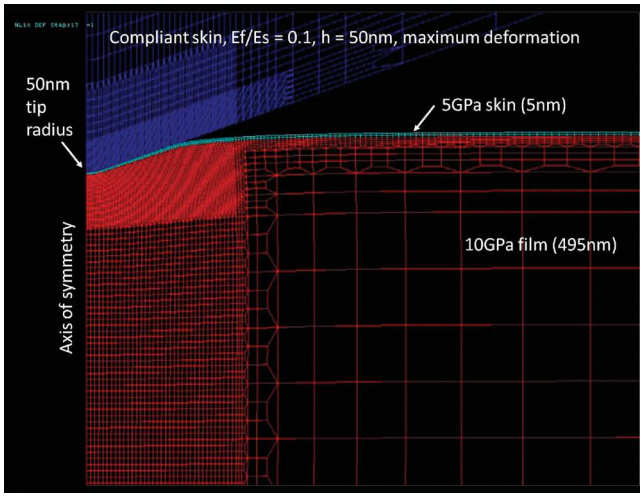

Figure 2. Deformed mesh for simulation 64. Tip radius and skin appear smaller relative to indentation depth.

		Maximum indenter displacement (h), nm							
E_{SL}, GPa	E_S, GPa	15	20	25	30	35	40	45	50
N/A	100	1	2	3	4	5	6	7	8
N/A	50	9	10	11	12	13	14	15	16
N/A	20	17	18	19	20	21	22	23	24
N/A	10	25	26	27	28	29	30	31	32
N/A	5	33	34	35	36	37	38	39	40
N/A	2	41	42	43	44	45	46	47	48
N/A	1	49	50	51	52	53	54	55	56
5	100	57	58	59	60	61	62	63	64
5	50	65	66	67	68	69	70	71	72
5	20	73	74	75	76	77	78	79	80
5	10	81	82	83	84	85	86	87	88
5	5	89	90	91	92	93	94	95	96
5	2	97	98	99	100	101	102	103	104
5	1	105	106	107	108	109	110	111	112
20	100	113	114	115	116	117	118	119	120
20	50	121	122	123	124	125	126	127	128
20	20	129	130	131	132	133	134	135	136
20	10	137	138	139	140	141	142	143	144
20	5	145	146	147	148	149	150	151	152
20	2	153	154	155	156	157	158	159	160
20	1	161	162	163	164	165	166	167	168

Table 1. Summary of finite-element simulations. Reference numbers for each simulation are shown in cells with shaded backgrounds. For example, the reference number 57 identifies the simulation of a 15nm indent into a film having a skin of modulus E_{SL} = 5GPa and a substrate of modulus E_S = 100GPa (E_f/E_S = 0.1).

These figures illustrate how the mesh is scaled according to the indentation depth. Although the tip radius was 50nm for both simulations, the tip radius appears smaller in Figure 2, because it is smaller, relative to indentation depth. Also, although the skin was 5nm in both simulations, it appears smaller in Figure 2, because it is smaller, relative to indentation depth. Thus, appropriate scaling of the finite-element model reveals what we know to be true in reality: imperfections, such as tip rounding and skins, become less influential with increasing indentation depth.

Analysis of Simulated Force-displacement Curves

Each simulation identified in Table 1 yielded a force-displacement curve which had to be further analyzed in order to achieve values of elastic modulus by either approach. The two approaches share a common analysis up to a point. This common analysis is explained first, followed by the analysis that is unique to each approach.

Common analysis

The analysis described in this section was applied to each simulation identified in Table 1. The first step in the analysis was to determine the contact stiffness (S) at the maximum displacement. (It should be recalled that these simulations were elastic, so only loading was simulated, and elastic analysis was applied to the loading process.) Logistically, contact stiffness was determined by fitting the force-displacement data to an analytic form and then differentiating and evaluating at the maximum displacement. (Note: only force-displacement pairs for which the force was greater than 50% of the peak force were included in the determination of the fit.)

The next step in the analysis was to determine the contact radius (a). The contact radius was determined as the radial position of the intersection of two lines: one defined by the last two nodes in contact (radially) and one defined by the first two nodes out of contact (radially). This method provided a smooth increase in contact radius, as opposed to discrete increments with each new contact node.

The apparent reduced modulus (E_{r-a}) was calculated from the stiffness and contact radius as:

$$E_{r-a} = S/(2\gamma a). \quad (1)$$

Without the correction factor (γ), Equation 1 is a derivative form of Sneddon's general equation relating force and displacement for contacting bodies. [5,6] Use of the correction factor gamma (γ) is not prescribed by ISO 14577, but it is necessary due to the fact that the boundary conditions used to derive the Sneddon stiffness equation are not quite appropriate for physical indentation experiments (or finite-element models of the same). [7] Expressions for γ have been proposed for both conical and paraboloid indenters; [7,8] the proposed forms are so similar that they can be consolidated to a single form, expressed in terms of the tangent to the indenter profile at the edge of contact, $f'(a)$. [8] (Note: $f(r)$ is the functional description of the profile of the indenter in terms of the radial coordinate, r.) The expression for γ used in this work was:

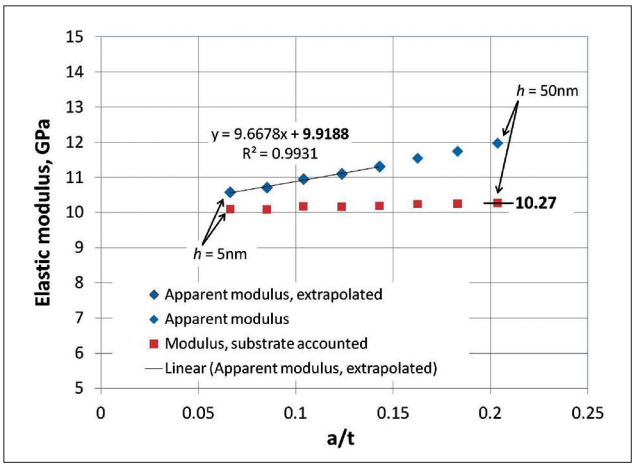

Figure 3. Results for simulations 1–8 (no skin, E_f/E_S = 0.1). Red symbols are obtained by applying the Hay-Crawford model to the blue symbols. Substrate-accounting approach yields a film modulus of 10.27GPa (2.7% greater than input value of 10GPa). Back-extrapolation approach yields a film modulus of 9.92GPa (0.8% less than the input value of 10GPa).

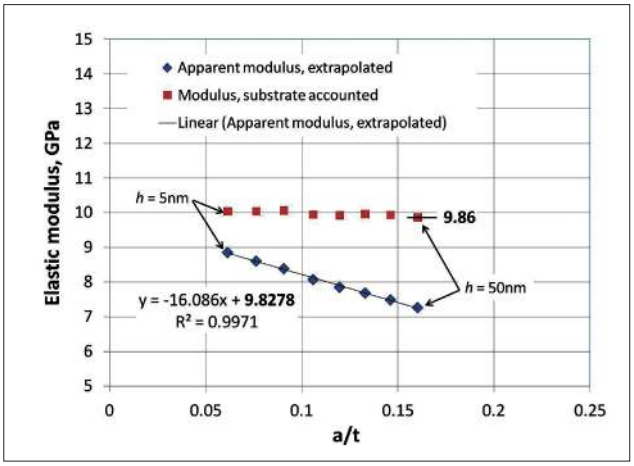

Figure 4. Results for simulations 41–48 (no skin, E_f/E_s = 5). Substrate-accounting approach yields a film modulus of 9.86 GPa (1.4% less than input value of 10 GPa). Back-extrapolation approach yields a film modulus of 9.83 GPa (1.7% less than the input value of 10 GPa).

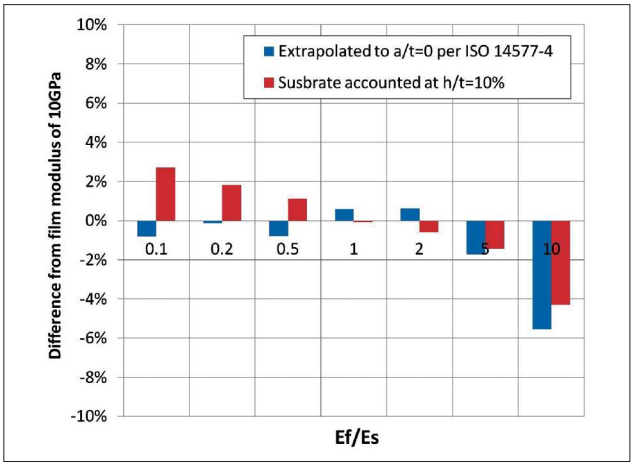

Figure 5. Summary of results for simulations 1–56 (no skin). Substrate-accounting approach (red bars) and back-extrapolation approach (blue bars) return the input modulus with similar accuracy. For 0.2 ≤ E_f/E_s ≤ 5, both approaches return the input modulus to within 2%, which is outstanding.

$$\gamma = 1 + f'(a)\,\frac{(1-2\nu)}{4(1-\nu)}, \qquad (2)$$

where ν represents the Poisson's ratio of the sample (ν = 0.25). The value of gamma resulting from this expression was between 1.056 and 1.060 for all simulations, the slight variation being due to the value of $f'(a)$ resulting from the prescribed indentation depth.

Next, the apparent modulus (E_a) was calculated from the apparent reduced modulus (E_{r-a}) as

$$E_a = (1-\nu^2)\left[\frac{1}{E_{r-a}} - \frac{1-\nu_i^2}{E_i}\right]^{-1}, \qquad (3)$$

where E_i and ν_i represent the properties of the indenter material (E_i = 1140 GPa and ν_i = 0.07). By this analysis, every simulation yielded exactly one value for apparent elastic modulus.

Subsequent analysis for the substrate-accounting approach

The apparent modulus, E_a, was converted to an apparent shear modulus, μ_a:

$$\mu_a = \frac{E_a}{2(1+\nu)}. \qquad (4)$$

Then the shear modulus of the film, μ_f, was calculated from the apparent shear modulus according to the Hay-Crawford model as[2]

$$\mu_f = \frac{-B + \sqrt{B^2 - 4AC}}{2A}, \text{ where} \qquad (5)$$

$$A = 0.0626(I_0)$$
$$B = \mu_S - [0.0626(I_0^2) - I_0 + 1]\mu_a$$
$$C = -I_0\,\mu_a\mu_S,$$

Finally, the Young's modulus of the film, E_f, was calculated from the shear modulus and Poisson's ratio as

$$E_f = 2\mu_f(1+\nu). \qquad (6)$$

By this analysis, every simulation yielded exactly one value of (substrate-accounted) film modulus. However, in order to compare this approach to the back-extrapolation approach, a single value of film modulus had to be obtained for each set of simulations on a particular "sample". Thus, the value of film modulus obtained by Equation 6 at the largest indentation depth for a particular "sample" was selected for comparison with the value obtained by the back-extrapolation approach. For example, simulations 17–24 are a set of simulations on a particular "sample." Although each of these simulations yielded a value of film modulus, the value obtained from the simulation to the largest indentation depth (simulation 24) was selected for comparison with the value obtained by the back-extrapolation approach.

Subsequent analysis for the back-extrapolation approach

For each set of simulations for a particular "sample" (say, for example, simulations 17–24), those values of apparent modulus determined by Equation 3 for which a/t was within the prescribed range were fit to the form of a line. The intercept of this line was taken to be the modulus of the film, E_f. For films which were more compliant than the substrate ($E_f/E_s \leq 1$), the range was $a/t < 1.5$. For films which were stiffer than the substrate ($E_f/E_s > 1$), the range was $a/t < 2.0$. In this way, each set of 8 simulations for a particular "sample" yielded one value for the modulus of the film, E_f.

Results and Discussion

Figure 3 shows the results for simulations 1–8. In this set of simulations, there was no skin; the film was mechanically uniform with an input modulus of 10 GPa. The substrate was ten times stiffer with an input modulus of 100 GPa. The blue diamonds represent the apparent modulus derived from each of the eight simulations. The left-most blue diamond represents the result for simulation 1 and the right-most blue diamond represents the result for simulation 8. As a function of normalized contact radius, the apparent modulus gradually increases due to the increasing influence of the stiff substrate. Five of these simulations had values for a/t which were within the prescribed range ($a/t < 1.5$); the linear fit to these five points is shown on the plot, with the intercept shown in bold font. The intercept of 9.92 GPa is the value of film modulus achieved by the back-extrapolation approach. This output value compares extremely well with the input value of 10 GPa. As explained

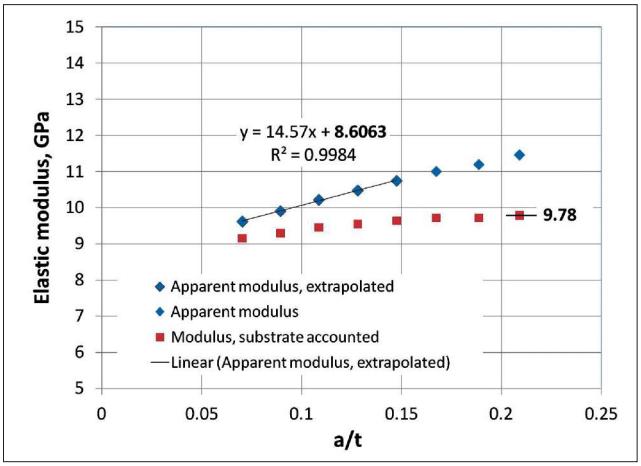

Figure 6. Results for simulations 57–64 (5 GPa skin, E_f/E_S = 0.1). Substrate-accounting approach yields a film modulus of 9.78 GPa (2.2% less than the input value of 10 GPa). Back-extrapolation approach yields a film modulus of 8.61 GPa (13.9% less than the input value of 10 GPa). Mechanical non-uniformity of the film is clearly evident in the substrate-accounted results.

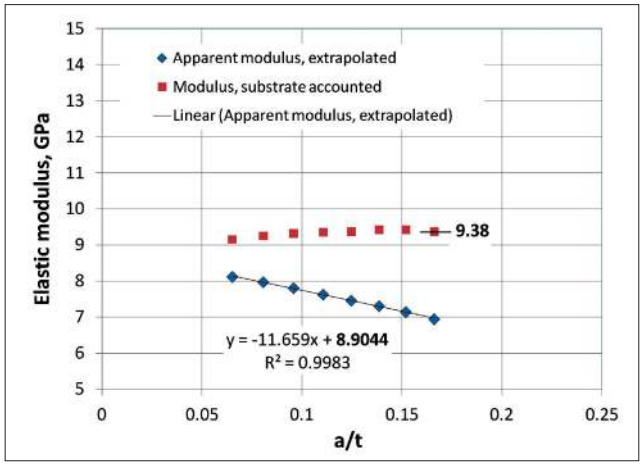

Figure 7. Results for simulations 97–104 (5 GPa skin, E_f/E_S = 5). Substrate-accounting approach yields a film modulus of 9.38 GPa (6.2% less than the input value of 10 GPa). Back-extrapolation approach yields a film modulus of 8.90 GPa (11.0% less than the input value of 10 GPa).

in the analysis section, the substrate-accounting approach further interprets the apparent modulus in order to obtain the film modulus. Thus, each red square represents a further interpretation of the value represented by the blue diamond at the same a/t. That is, each red square is a "substrate-accounted" version of the corresponding blue diamond. The left-most red square represents the result for simulation 1 and the right-most red square represents the result for simulation 8. Because the red squares represent values that have been substrate-accounted, they manifest a nearly constant value with increasing a/t. A very slight upward trend exists because the Hay-Crawford model is conservative—it always under-predicts the influence of the substrate and thus never over-corrects the results. The value of 10.27 GPa—the value obtained from the last simulation in this set—is the value of film modulus achieved by the substrate-accounting approach. Thus, for this set of simulations, the back-extrapolation approach yields a value for film modulus that is closer to the input value of 10 GPa than the substrate-accounting approach.

Figure 4, which shows the results from simulations 41–48, should be interpreted in the same way as Figure 3. For these simulations, the film was five times stiffer than the substrate, and the apparent moduli (blue diamonds) manifest the influence of the substrate with increasing a/t. Again, the slight downward trend in the substrate-accounted moduli (red squares) is due to the conservative nature of the Hay-Crawford model. For this set of simulations, the two approaches return virtually equivalent values for film modulus.

Figure 5 summarizes all results for simulations 1–56. Each bar represents the relative difference between the output and input film modulus for a particular approach. The two values of film modulus identified in Figure 3 are represented by the first two bars (for E_f/E_S = 0.1) of Figure 5. The two values of film modulus identified in Figure 4 are represented by the sixth set of bars (for E_f/E_S = 5). When the film is uniform, both approaches return the input value with about the same degree of accuracy. However, the substrate-accounting approach does have a practical advantage in that a value for film modulus can be achieved with a single test. Of course in the experimental realm, repetition is needed to achieve and quantify reliability, but the necessary repetition for the substrate-accounting approach will be less than the necessary repetition for the back-extrapolation approach under the same circumstances. (Note: Although ISO 14577-4 requires 15 measurements at three different values of a/t for this analysis, it recommends using at least 50 measurements at 5 or more different values of a/t.)

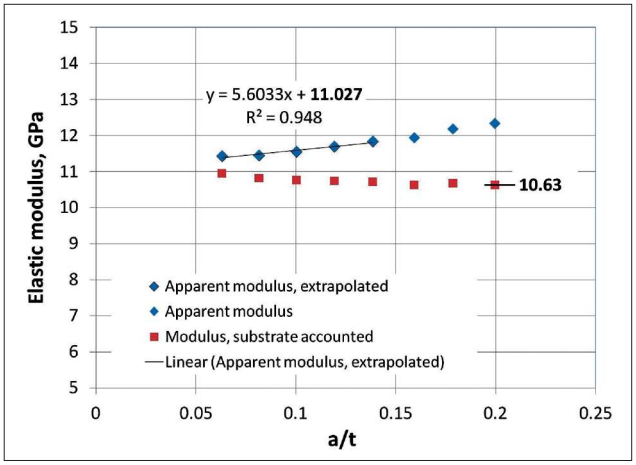

Figure 8. Results for simulations 113–120 (20 GPa skin, E_f/E_S = 0.1). Substrate-accounting approach yields a film modulus of 10.63 GPa (6.3% greater than the input value of 10 GPa). Back-extrapolation approach yields a film modulus of 11.027 GPa (10.0% greater than the input value of 10 GPa).

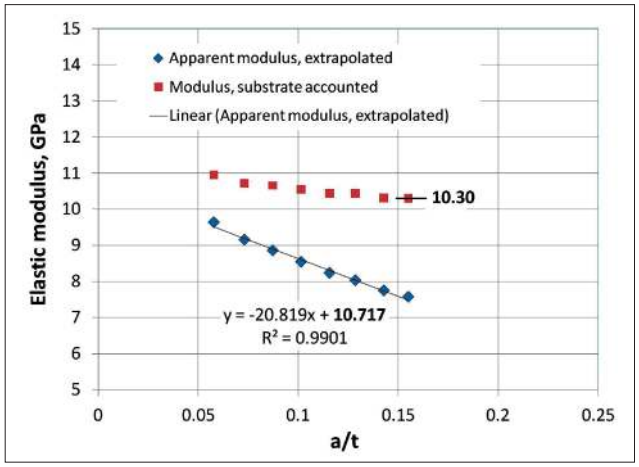

Figure 9. Results for simulations 153–160 (20 GPa skin, E_f/E_S = 5). Substrate-accounting approach yields a film modulus of 10.30 GPa (3.0% greater than the input value of 10 GPa). Back-extrapolation approach yields a film modulus of 10.72 GPa (7.2% greater than the input value of 10 GPa).

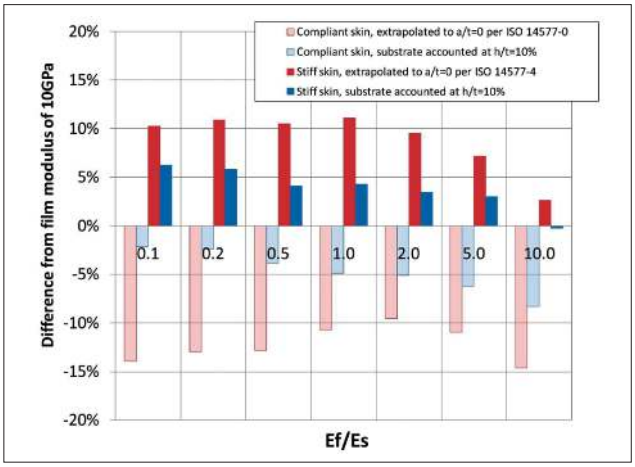

Figure 10. Summary of results for simulations 57–168. Plotted values may be found in Table 2. In the presence of a skin that is mechanically different from the rest of the film, the substrate-accounting approach (blue bars) returns the input modulus of the film with superior accuracy.

Figure 6, which shows the results from simulations 57–64, should be interpreted in the same way as Figure 3. Indeed, Figure 6 should be compared closely with Figure 3, because the only difference between the two sets of simulations is the presence of a 5 nm-thick compliant skin. In Figure 6, the apparent moduli (blue diamonds) manifest the influence of both the skin and the substrate. Because the skin has the most significant effect at small a/t, the value of film modulus achieved by extrapolating to a/t = 0 is low relative to the input modulus of the film. Because the red squares represent substrate-accounted values, they "level-off" near the input value with increasing a/t. In this case, substrate-accounting has two benefits. First, the film modulus can be accurately obtained simply by indenting to a depth that is significantly greater than the thickness of the skin. Indentation depth is not critically important, but it should be noted that the Hay-Crawford model has not been verified for indentation depths greater than 40% of the film thickness. Second, the presence of the skin is more obvious in the substrate-accounted values than in the apparent values. The increase in the substrate-accounted values with increasing a/t notifies the experimenter that something is different at the surface of the film. It would be difficult to draw such a conclusion from the apparent modulus alone, because the eye tends to attribute the entirety of the increase to substrate influence.

In the same way, Figure 7 should be compared to Figure 4, because the only difference between the two sets of simulations is the presence of a compliant skin. Figures 8 and 9 should also be compared to Figures 3 and 4, respectively, in order to see the effect of a stiff skin.

It should be noted that when the skin is stiffer than the film and the substrate is more compliant (or vice versa), the results for either approach tend to be fortuitously good, because the two sources of difference cancel each other out to some degree. That is, the stiff skin compensates for the compliant substrate, making the output film modulus fortuitously close to the input. This phenomenon is clearly evident in Figure 9. However, when the skin and the substrate are both more stiff (or more compliant) than the film, the two sources of difference compound—the results in Figure 8 are exemplary in this respect.

Table 2 and Figure 10 summarize all results for simulations which included a skin. From Figure 10, it is clear that if the film has a skin, the substrate-accounting

		5 GPa skin (5 nm) on 10 GPa film (495 nm)				20 GPa skin (5 nm) on 10 GPa film (495 nm)			
		Extrapolated to a/t=0 per ISO 14577-4		Substrate accounted at h/t=10%		Extrapolated to a/t=0 per ISO 14577-4		Substrate accounted at h/t=10%	
E_s	E_f/E_s	Value	$(E-E_f)/E_f$	Value	$(E-E_f)/E_f$	Value	$(E-E_f)/E_f$	Value	$(E-E_f)/E_f$
GPa		N/m	%	N/m	%	N/m	%	N/m	%
100	0.1	8.606	-13.94%	9.782	-2.18%	11.027	10.27%	10.626	6.26%
50	0.2	8.702	-12.98%	9.755	-2.45%	11.089	10.89%	10.580	5.80%
20	0.5	8.719	-12.81%	9.612	-3.88%	11.049	10.49%	10.409	4.09%
10	1.0	8.932	-10.68%	9.513	-4.87%	11.107	11.07%	10.429	4.29%
5	2.0	9.044	-9.56%	9.491	-5.09%	10.952	9.52%	10.346	3.46%
2	5.0	8.904	-10.96%	9.375	-6.25%	10.717	7.17%	10.300	3.00%
1	10.0	8.537	-14.63%	9.169	-8.31%	10.261	2.61%	9.975	-0.25%

Table 2. Summary of results for films with skins (simulations 57–168). Relative differences from input value of film modulus are plotted in Figure 10.

approach is much better for obtaining the elastic modulus of the "bulk" of the film.

Conclusions

It should be remembered that although the two approaches considered in this work have fundamental differences, they are not mutually exclusive. The two approaches are extensions of the same underlying analysis. One is not forced to choose between them, because both approaches can be followed for the same data set. However, the substrate-accounting approach adds significant value. First, in situations where the film is mechanically uniform, a value of film modulus is achieved with every test, and the indentation depth is not critically important. Second, if the film has a skin, its presence is more easily discerned if the moduli are substrate-accounted. Moreover, the substrate-accounting approach returns a value for film modulus that is closer to the value for the bulk of the film. For best results, the indentation depth should be large relative to the thickness of the skin, but still less than 40% of the film thickness.

References

1. Oliver, W.C. and Pharr, G.M., "An Improved Technique for Determining Hardness and Elastic-Modulus Using Load and Displacement Sensing Indentation Experiments," Journal of Materials Research 7(6), 1564–1583, 1992.

2. Hay, J.L. and Crawford, B., "Measuring Substrate-Independent Modulus of Thin Films," Journal of Materials Research 26(6), 2011.

3. Hay, J.L., Measuring Substrate-Independent Young's Modulus. NMO Application Notes, August 31, 2014 [cited February, 24 2011]; Available from: http://literature.cdn.keysight.com/litweb/pdf/5990-6507EN.pdf.

4. ISO/FDIS 14577-4:"Metallic materials – Instrumented indentation test for hardness and materials parameters – Part 4: Test method for metallic and non-metallic coatings."

5. Sneddon, I.N., "The Relation Between Load and Penetration in the Axisymmetric Boussinesq Problem for a Punch of Arbitrary Profile," Int. J. Eng. Sci. 3(1), 47–57, 1965.

6. Pharr, G.M., Oliver, W.C., and Brotzen, F.R., "On the Generality of the Relationship among Contact Stiffness, Contact Area, and Elastic-Modulus during Indentation," Journal of Materials Research 7(3), 613–617, 1992.

7. Hay, J.C., Bolshakov, A., and Pharr, G.M., "A Critical Examination of the Fundamental Relations Used in the Analysis of Nanoindentation Data," Journal of Materials Research 14(6), 2296–2305 1999.

8. Hay, J.L. and Wolff, P.J., "Small Correction Required When Applying the Hertz Contact Model to Instrumented Indentation Data," Journal of Materials Research 16(5), 1280–1286, 2001.

Nanomeasurement Systems from Keysight Technologies

Keysight Technologies, Inc., the premier measurement company, offers high precision instruments for nanoscience research in academia and industry. Exceptional worldwide support is provided by experienced application scientists and technical service personnel. Keysight's leading-edge R&D laboratories ensure the continued, timely introduction and optimization of innovative, easy-to-use nanomeasurement system technologies.

For more information on Keysight Technologies' products, applications or services, please contact your local Keysight office. The complete list is available at: www.keysight.com/find/contactus

Americas

Canada	(877) 894 4414
Brazil	55 11 3351 7010
Mexico	001 800 254 2440
United States	(800) 829 4444

Asia Pacific

Australia	1 800 629 485
China	800 810 0189
Hong Kong	800 938 693
India	1 800 112 929
Japan	0120 (421) 345
Korea	080 769 0800
Malaysia	1 800 888 848
Singapore	1 800 375 8100
Taiwan	0800 047 866
Other AP Countries	(65) 6375 8100

Europe & Middle East

Austria	0800 001122
Belgium	0800 58580
Finland	0800 523252
France	0805 980333
Germany	0800 6270999
Ireland	1800 832700
Israel	1 809 343051
Italy	800 599100
Luxembourg	+32 800 58580
Netherlands	0800 0233200
Russia	8800 5009286
Spain	800 000154
Sweden	0200 882255
Switzerland	0800 805353 Opt. 1 (DE) Opt. 2 (FR) Opt. 3 (IT)
United Kingdom	0800 0260637

For other unlisted countries:
www.keysight.com/find/contactus
(BP-09-23-14)

www.keysight.com/find/nano

KEYSIGHT TECHNOLOGIES

Published in USA, August 1, 2014
5990-9003EN
www.keysight.com